J|A|C|S ARTICLES

Published on Web 02/05/2010

Formation of the Phenyl Radical [$C_6H_5(X^2A_1)$] under Single Collision Conditions: A Crossed Molecular Beam and ab Initio Study

Fangtong Zhang,[†] Brant Jones,[†] Pavlo Maksyutenko,[†] Ralf I. Kaiser,*[,†] Christine Chin,[‡] Vadim V. Kislov,[‡] and Alexander M. Mebel*[,‡]

Department of Chemistry, University of Hawai'i, Honolulu, Hawaii 96822, and Department of Chemistry and Biochemistry, Florida International University, Miami, Florida 33199

Received October 7, 2009; E-mail: ralfk@hawaii.edu; mebela@fiu.edu

Abstract: Reactions of dicarbon molecules (C_2) with C_4H_6 isomers such as 1,3-butadiene represent a potential, but hitherto unnoticed, route to synthesize the first aromatic C_6 ring in hydrocarbon flames and in the interstellar medium where concentrations of dicarbon transient species are significant. Here, crossed molecular beams experiments of dicarbon molecules in their $X^1\Sigma_g^+$ electronic ground state and in the first electronically excited $a^3\Pi_u$ state have been conducted with 1,3-butadiene and two partially deuterated counterparts (1,1,4,4-D4-1,3-butadiene and 2,3-D2-1,3-butadiene) at two collision energies of 12.7 and 33.7 kJ mol^{-1}. Combining these scattering experiments with electronic structure and RRKM calculations on the singlet and triplet C_6H_6 surfaces, our investigation reveals that the aromatic phenyl radical is formed predominantly on the triplet surface via indirect scattering dynamics through a long-lived reaction intermediate. Initiated by a barrierless addition of triplet dicarbon to one of the terminal carbon atoms of 1,3-butadiene, the collision complex undergoes trans−cis isomerization followed by ring closure and hydrogen migration prior to hydrogen atom elimination, ultimately forming the phenyl radical. The latter step emits the hydrogen atom almost perpendicularly to the rotational plane of the decomposing intermediate and almost parallel to the total angular momentum vector. On the singlet surface, smaller contributions of phenyl radical could not be excluded; experiments with partially deuterated 1,3-butadiene indicate the formation of the thermodynamically less stable acyclic $H_2CCHCCCCH_2$ isomer. This study presents the very first experimental evidence, contemplated by theoretical studies, that under single collision conditions an aromatic hydrocarbon molecule can be formed in a bimolecular gas-phase reaction via reaction of two acyclic molecules involving cyclization processes at collision energies highly relevant to combustion flames.

1. Introduction

Polycyclic aromatic hydrocarbons (PAHs) and soot particles are of fundamental importance in combustion processes as well as in atmospheric and interstellar chemistry. For instance, PAHs and soot generated during the combustion of fossil fuels are recognized as the major source of airborne pollutants,[1] as many of them are carcinogenic.[2] Nanosized PAH species also contribute significantly to the global warming on Earth[3] and play a crucial role in the ongoing chemistry of the organic haze layers as present in the atmosphere of Saturn's moon Titan.[4] Considering interstellar environments, PAHs are thought to account for up to 30% of the carbon in the galaxy and may provide nucleation sites for the formation of carbonaceous dust particles.[5] Therefore, an understanding of the underlying formation mechanisms of PAHs and soot particles is essential to the combustion, atmospheric, and astrochemistry communities. After decades of detailed studies, it is now widely accepted that the first critical step toward the formation of complex PAHs and soot particles is the synthesis of the first aromatic ring molecule: benzene $C_6H_6(X^1A_{1\,g})$ and/or the phenyl radical $C_6H_5(X^2A_1)$.[6] Hereafter, complex PAHs can be formed via hydrogen abstraction and acetylene addition (HACA) sequences,[7] through phenyl addition and cyclization pathways (PAC),[8] or via the newly proposed barrierless ethynyl addition mechanism (EAM).[9]

A range of reaction mechanisms have been recommended to form the very first aromatic ring species. Considering even-carbon-atom pathways, reactions of n-C_4H_3 and the n-C_4H_5

[†] University of Hawai'i.
[‡] Florida International University.

(1) Kunzli, N.; Kaiser, R.; Medina, S.; Studnicka, M.; Chanel, O.; Filliger, P.; Herry, M.; Horak, F., Jr.; Puybonnieux-Texier, V.; Quenel, P.; Schneider, J.; Seethaler, R.; Vergnaud, J. C.; Sommer, H. *Lancet* **2000**, *356*, 795.
(2) Denissenko, M. F.; Pao, A.; Tang, M.-s.; Pfeifer, G. P. *Science* **1996**, *274*, 430.
(3) Violi, A.; Venkatnathan, A. *J. Chem. Phys.* **2006**, *125*, 054302/1.
(4) Sagan, C.; Khare, B. N.; Thompson, W. R.; McDonald, G. D.; Wing, M. R.; Bada, J. L.; Tuan Vo, D.; Arakawa, E. T. *Astrophys. J.* **1993**, *414*, 399.
(5) Cook, D. J.; Schlemmer, S.; Balucani, N.; Wagner, D. R.; Steiner, B.; Saykally, R. J. *Nature (London)* **1996**, *380*, 227.
(6) Richter, H.; Howard, J. B. *Prog. Energy Combust. Sci.* **2000**, *26*, 565.
(7) Bockhorn, H.; Fetting, F.; Heddrich, A.; Wannemacher, G. *Ber. Bunsen-Ges. Phys. Chem.* **1987**, *91*, 819.
(8) Shukla, B.; Susa, A.; Miyoshi, A.; Koshi, M. *J. Phys. Chem. A* **2008**, *112*, 2362.
(9) Mebel, A. M.; Kislov, V. V.; Kaiser, R. I. *J. Am. Chem. Soc.* **2008**, *130*, 13618.

10.1021/ja908559v

radicals with acetylene (C_2H_2) have been proposed to synthesize the first six-membered aromatic rings in combustion flames, that is, the phenyl radical (C_6H_5; reaction 1) and benzene (C_6H_6, reaction 2; term symbols have been omitted for clarity).[10−12] A recent model by Richter and Howard[13] proposed that an addition of the vinyl (C_2H_3) radical to vinylacetylene (C_4H_4) followed by successive isomerization steps can also lead to benzene plus a hydrogen atom (reaction 3). Miller and Melius[14] as well as Kern and Xie[15] suggested alternative odd-carbon-atom reaction pathways involving the recombination of two propargyl radicals (C_3H_3, reaction 4). Electronic structure calculations imply that the initially formed acyclic collision complex(es) of the recombination of two propargyl radicals can isomerize via multisteps to ultimately form benzene and/or the phenyl radical plus a hydrogen atom.[16] Further odd-carbon-atom reaction sequences may also involve the reaction of C_5H_5 isomers with the methyl radical (CH_3, reaction 5).[17] An alternative even−odd-carbon-atom sequence could include the reaction of propargyl radicals (C_3H_3) with acetylene (C_2H_2) to yield the cyclopentadienyl radical (C_5H_5, reaction 6). The latter can react in multiple steps to form benzene[18] or naphthalene.[19] On the other hand, the formation of the first six-membered aromatic ring can proceed at higher pressures via isomerization of acyclic C_6H_x isomers ($x = 4-6$).[20,21] For completeness, it should be also pointed out that the synthesis of benzene or of the phenyl radical may not necessarily be the rate-limiting step in the growth of polycyclic hydrocarbon molecules. Here, PAHs could form without involving six-membered aromatic precursors via reactions of polyacetylenes with C_4H_x species ($x = 1-5$)[22−25] and through reactions of two C_5H_5 radicals followed by rearrangements and hydrogen emission(s) to form naphthalene and/or the azulene isomer.[19]

$$n\text{-}C_4H_3 + C_2H_2 \rightarrow C_6H_5 \text{ even} \quad (1)$$

$$n\text{-}C_4H_5 + C_2H_2 \rightarrow C_6H_6 + H \text{ even} \quad (2)$$

$$C_4H_4 + C_2H_3 \rightarrow C_6H_6 + H \text{ even} \quad (3)$$

$$C_3H_3 + C_3H_3 \rightarrow C_6H_6//C_6H_5 + H \text{ odd} \quad (4)$$

$$C_5H_5 + CH_3 \rightarrow C_6H_6 + H + H \text{ odd} \quad (5)$$

$$C_3H_3 + C_2H_2 \rightarrow c\text{-}C_5H_5 \text{ even−odd} \quad (6)$$

However, reactions of dicarbon in its electronic ground and first excited states, that is, $C_2(X^1\Sigma_g^+)$ and $C_2(a^3\Pi_u)$, with C_4H_6 isomers, that is, 1,3-butadiene, 1,2-butadiene, 1-butyne, and 2-butyne (dimethylacetylene), present a potential alternative to the proposed reaction sequences 1−6 in those environments with significant concentrations of dicarbon transient species. Here, dicarbon molecules react with C_4H_6 isomers to form C_6H_6 intermediates; in combustion flames, these intermediates either can be stabilized, isomerized prior to their stabilization to acyclic structures, or fragment via atomic and/or molecular hydrogen loss, forming C_6H_5 isomers such as phenyl and C_6H_4 structures such as didehydrobenzenes. In the interstellar medium, where single collision conditions dominate, the intermediates fragment to the products or decompose back to the reactants. It should be stressed that C_4H_6 isomers have been observed in hydrocarbon flames. Utilizing the Advanced Light Source in Berkeley, Cool et al. probed, for instance, the 1,3-butadiene isomer via photoionization mass spectrometry using tunable vacuum ultraviolet photons from 8.5 to 10.0 eV.[26] Here, 1,3-butadiene was detected in cyclohexane,[27] isobutene,[28] heptane,[29] ethane,[30] and methane flames.[31] Note that 1,3-butadiene can exist in its *s-cis* and *s-trans* forms; the latter is more stable by about 12 kJ mol^{-1} as compared to the *s-cis* isomer. These structures are not classical cis and trans forms, because the *s-cis* and *s-trans* conformations of 1,3-butadiene can be interconverted via rotation about the carbon−carbon single bond (hence the prefix *s*).[32] At flame temperatures of up to 3000 K, up to 60% of the 1,3-butadiene molecules prevail in its cis form. Most importantly, C_4H_6 isomers can be also interconverted via hydrogen atom addition−hydrogen atom elimination pathways. For instance, a recent investigation of the unimolecular decomposition of the 1-buten-2-yl radical, $H_2CCC_2H_5$, verified the formation of the 1-butyne and 1,2-butadiene isomers via an atomic hydrogen emission.[33] Therefore, a reversed reaction sequence is expected to convert a significant fraction of 1-butyne to the 1,2-butadiene isomer via atomic hydrogen addition−elimination pathways.

Also, the dicarbon reactant presents the simplest representative of a bare carbon molecule. Dicarbon species have been identified in their electronic ground states in high temperature combustion flames under fuel-rich conditions of incipient soot

(10) Frenklach, M. *Phys. Chem. Chem. Phys.* **2002**, *4*, 2028.
(11) Bittner, J. D.; Howard, J. B. *Symp. (Int.) Combust., [Proc.]* **1981**, *18*, 1105.
(12) Frenklach, M.; Clary, D. W.; Gardiner, W. C., Jr.; Stein, S. E. *Symp. (Int.) Combust., [Proc.]* **1985**, *20*, 887.
(13) Richter, H.; Howard, J. B. *Phys. Chem. Chem. Phys.* **2002**, *4*, 2038.
(14) Miller, J. A.; Melius, C. F. *Combust. Flame* **1992**, *91*, 21.
(15) Kern, R. D.; Xie, K. *Prog. Energy Combust. Sci.* **1991**, *17*, 191.
(16) Melius, C. F.; Miller, J. A.; Evleth, E. M. *Symp. (Int.) Combust., [Proc.]* **1992**, *24*, 621.
(17) Ikeda, E.; Tranter, R. S.; Kiefer, J. H.; Kern, R. D.; Singh, H. J.; Zhang, Q. *Proc. Combust. Inst.* **2000**, *28*, 1725.
(18) Moskaleva, L. V.; Mebel, A. M.; Lin, M. C. *Symp. (Int.) Combust., [Proc.]* **1996**, *26*, 521.
(19) Kislov, V. V.; Mebel, A. M. *J. Phys. Chem. A* **2007**, *111*, 9532.
(20) Kazakov, A.; Wang, H.; Frenklach, M. *Combust. Flame* **1995**, *100*, 111.
(21) Yoshihara, Y.; Kazakov, A.; Wang, H.; Frenklach, M. *Symp. (Int.) Combust., [Proc.]* **1994**, *25*, 941.
(22) Bockhorn, H.; Fetting, F.; Wenz, H. W. *Ber. Bunsen-Ges. Phys. Chem.* **1983**, *87*, 1067.
(23) McEnally, C. S.; Pfefferle, L. D.; Robinson, A. G.; Zwier, T. S. *Combust. Flame* **2000**, *123*, 344.
(24) Arrington, C. A.; Ramos, C.; Robinson, A. D.; Zwier, T. S. *J. Phys. Chem. A* **1998**, *102*, 3315.
(25) Cavallotti, C.; Fascella, S.; Rota, R.; Carra, S. *Combust. Sci. Technol.* **2004**, *176*, 705.
(26) Cool, T. A.; Nakajima, K.; Mostefaoui, T. A.; Qi, F.; McIlroy, A.; Westmoreland, P. R.; Law, M. E.; Poisson, L.; Peterka, D. S.; Ahmed, M. *J. Chem. Phys.* **2003**, *119*, 8356.
(27) El Bakali, A.; Braun-Unkhoff, M.; Dagaut, P.; Frank, P.; Cathonnet, M. *Proc. Combust. Inst.* **2000**, *28*, 1631.
(28) Dagaut, P.; Cathonnet, M. *Combust. Sci. Technol.* **1998**, *137*, 237.
(29) Li, S. C.; Williams, F. A. *Proc. Combust. Inst.* **2000**, *28*, 1031.
(30) Melton, T. R.; Inal, F.; Senkan, S. M. *Combust. Flame* **2000**, *121*, 671.
(31) Melton, T. R.; Vincitore, A. M.; Senkan, S. M. *Symp. (Int.) Combust., [Proc.]* **1998**, *27*, 1631.
(32) Solomons, G.; Fryhle, C. *Organic Chemistry*, 7th ed.; John Wiley & Sons, Inc.: New York, 2000.
(33) Miller, J. L.; Krisch, M. J.; Butler, L. J.; Shu, J. *J. Phys. Chem. A* **2005**, *109*, 4038.

formation and in chemical vapor deposition processes at concentrations up to 10^{15} cm^{-3}.[34−36] Most importantly, dicarbon molecules were also detected in hydrocarbon flames and CVD processes at high concentrations not only in the electronic ground state, but also in their first electronically excited state, that is, $a^3\Pi_u$, which lies 8.6 kJ mol^{-1} above the ground state.[37−41] In low pressure hydrocarbon flames, spectroscopic investigations of the Swan band system[42−44] suggest concentrations of dicarbon in its $a^3\Pi_u$ state of $10^{13}-10^{14}$ cm^{-3} at flame temperatures ranging from 1500 to 1900 K.[45] Recent in situ probing of the $a^3\Pi_u$ state at temperatures of 1200 K indicate that due to the higher degeneracy of the triplet population, about 75% or more of dicarbon molecules exist in their $a^3\Pi_u$ state.[42,46]

Because of the potential importance of dicarbon reactions with C_4H_6 isomers to possibly form the phenyl radical and/or its acyclic isomers, we conducted a combined crossed molecular beam and ab initio study on the gas-phase reactions of dicarbon in its ground ($X^1\Sigma_g^+$) and first electronic excited state ($a^3\Pi_u$) with the thermodynamically most stable C_4H_6 isomer, 1,3-butadiene, together with its partially deuterated isotopomers under single collision conditions. Note that previous kinetic[47,48] and crossed beams studies[49] of dicarbon reactions with unsaturated hydrocarbons like acetylene (C_2H_2, $X^1\Sigma_g^+$),[50] ethylene (C_2H_4, X^1A_g),[51] methylacetylene (CH_3CCH, X^1A_1),[52] and allene (H_2CCCH_2, X^1A_1)[53] suggested that these reactions are rapid, proceed without entrance barriers through indirect scattering dynamics, and are exoergic with no transition states lying higher in energy than the separate reactants. Because of the barrierless nature of these processes, the reactions of dicarbon have also been suggested to be important in low temperature environments such as cold molecular clouds and in the atmosphere of Saturn's moon Titan where dicarbon might exist as a transient species formed via photodissociation of the ethynyl (CCH) radical.[49,54] Under single collision conditions, the exchange of a hydrogen atom by dicarbon has been found to be the dominant reaction channel in the reactions of both ground- and excited-state dicarbon molecules with unsaturated hydrocarbon molecules.[55] Therefore, it is logical to predict that the reaction of dicarbon molecules with 1,3-butadiene shall lead to the formation of radicals of the generic formula C_6H_5 plus hydrogen atoms via C_6H_6 intermediates. However, what are the underlying reaction mechanisms? Is it possible that the aromatic phenyl radical is formed in this reaction? In this context, it is important to note that the singlet C_6H_6 potential energy surface (PES) has been well studied.[56,57] These investigations mostly focused on different C_6H_6 isomers (217 in total). However, the excited C_6H_6 triplet surface has received much less attention. Therefore, we also carried out high level electronic structure calculations on the parts of the relevant singlet and triplet C_6H_6 potential energy surfaces, which are relevant to the dicarbon plus 1,3-butadiene reactions.

Table 1. Peak Velocities (v_p) of the Intersecting Segments of the Supersonic Beams Together with the Corresponding Collision Energies (E_c) and Center-of-Mass Angles (Θ_{CM}), That Is, the Laboratory Angle of the Center-of-Mass Velocity Vector[a]

beam	v_p (ms^{-1})	E_c, kJ mol^{-1}	Θ_{CM}	E_T/E_{Max} (%)
$CH_2CHCHCH_2(X^1A_g)$	770 ± 30			
$C_2(X^1\Sigma_g^+/a^3\Pi_u)$/Ne	970 ± 20	12.7 ± 0.4	60.7 ± 0.5	27.7 ± 2.0
$C_2(X^1\Sigma_g^+/a^3\Pi_u)$/He	1860 ± 20	33.7 ± 0.6	43.0 ± 0.5	27.8 ± 2.0
$CD_2CHCHCD_2(X^1A_g)$	760 ± 30			
$C_2(X^1\Sigma_g^+/a^3\Pi_u)$/Ne	970 ± 20	12.9 ± 0.4	62.2 ± 0.5	
$CH_2CDCDCH_2(X^1A_g)$	760 ± 30			
$C_2(X^1\Sigma_g^+/a^3\Pi_u)$/Ne	970 ± 20	12.8 ± 0.4	61.3 ± 0.5	

[a] Also indicated are the fractions of total energy that channeled into the translational degrees of freedom the reaction products (E_T/E_{Max}). The peak velocity defined the distribution maximum of the velocity distribution of the supersonic beam.

2. Experimental Setup and Data Analysis

The crossed beam reactions of dicarbon [$C_2(X^1\Sigma_g^+/a^3\Pi_u)$] with 1,3-butadiene [$CH_2CHCHCH_2$ (X^1A_g)] were conducted in a universal crossed molecular beams machine under single collision conditions.[58−61] Briefly, a pulsed dicarbon beam was generated in the primary source chamber by laser ablation of a graphite rod at 266 nm at 30 Hz and 5−10 mJ per pulse.[62] The ablated species were seeded in neat carrier gas (neon or helium; 99.9999%; 4 atm; Gaspro) released by a Proch-Trickl pulsed valve at pulse widths of 80 μs and driving voltages of −400 V. After passing a skimmer, a four-slot chopper wheel selected a part out of the dicarbon beam with a well-defined velocity (Table 1). This segment of the dicarbon beam crossed a pulsed, neat 1,3-butadiene beam ($CH_2CHCHCH_2$,

(34) Gordon, A. G. *The Spectroscopy of Flames*; Chapman and Hall Ltd./Wiley: New York, 1974.
(35) Rennick, C. J.; Smith, A. G.; Smith, J. A.; Wills, J. B.; Orr-Ewing, A. J.; Ashfold, M. N. R.; Mankelevich, Y. A.; Suetin, N. V. *Diamond Relat. Mater.* **2004**, *13*, 561.
(36) Hiramatsu, M.; Kato, K.; Lau, C. H.; Foord, J. S.; Hori, M. *Diamond Relat. Mater.* **2003**, *12*, 365.
(37) Rennick, C. J.; Smith, J. A.; Ashfold, M. N. R.; Orr-Ewing, A. J. *Chem. Phys. Lett.* **2004**, *383*, 518.
(38) Wang, H.; Zhu, Z.; Zhang, S.; Pei, L.; Chen, Y. *Chem. Phys. Lett.* **2005**, *407*, 217.
(39) Sherrill, C. D.; Piecuch, P. *J. Chem. Phys.* **2005**, *122*, 124104/1.
(40) Toffoli, D.; Lucchese, R. R. *J. Chem. Phys.* **2004**, *120*, 6010.
(41) Okada, A.; Kijima, K. *J. Phys. D: Appl. Phys.* **2002**, *35*, 2126.
(42) Smith, G. P.; Park, C.; Schneiderman, J.; Luque, J. *Combust. Flame* **2005**, *141*, 66.
(43) Nyholm, K.; Kaivola, M.; Aminoff, C. G. *Opt. Commun.* **1994**, *107*, 406.
(44) Goldsmith, J. E. M.; Kearsley, D. T. B. *Appl. Phys. B: Laser Opt.* **1990**, *B50*, 371.
(45) Hino, Y.; Suzukawa, Y.; Ishiguro, T.; Mori, I.; Kitagawa, K.; Sugiyama, S.; Konishi, N.; Arai, N. *Int. Jt. Power Gener. Conf.: Power Fuels Combust. Technol. Nucl. Eng., Proc.* **2000**, 613.
(46) Chase, M. W., Jr.; Davies, C. A.; Downey, J. R., Jr.; Frurip, D. J.; McDonald, R. A.; Syverud, A. N. *J. Phys. Chem. Ref. Data, Suppl.* **1985**, *14*, 646.
(47) Pitts, W. M.; Pasternack, L.; McDonald, J. R. *Chem. Phys.* **1982**, *68*, 417.
(48) Pasternack, L.; Pitts, W. M.; McDonald, J. R. *Chem. Phys.* **1981**, *57*, 19.
(49) Gu, X.; Guo, Y.; Zhang, F.; Mebel, A. M.; Kaiser, R. I. *Faraday Discuss.* **2006**, *133*, 245.
(50) Gu, X.; Guo, Y.; Mebel, A. M.; Kaiser, R. I. *J. Phys. Chem. A* **2006**, *110*, 11265.
(51) Gu, X.; Guo, Y.; Zhang, F.; Mebel, A. M.; Kaiser, R. I. *Chem. Phys.* **2007**, *335*, 95.
(52) Guo, Y.; Gu, X.; Balucani, N.; Kaiser, R. I. *J. Phys. Chem. A* **2006**, *110*, 6245.
(53) Guo, Y.; Gu, X.; Zhang, F.; Mebel, A. M.; Kaiser, R. I. *J. Phys. Chem. A* **2006**, *110*, 10699.
(54) Canosa, A.; Paramo, A.; Le Picard, S. D.; Sims, I. R. *Icarus* **2007**, *187*, 558.
(55) Gu, X.; Kaiser, R. I.; Mebel, A. M. *ChemPhysChem* **2008**, *9*, 350.
(56) Dinadayalane, T. C.; Priyakumar, U. D.; Sastry, G. N. *J. Phys. Chem. A* **2004**, *108*, 11433.
(57) Bettinger, H. F.; Schreiner, P. R.; Schaefer, H. F., III; Schleyer, P. v. R. *J. Am. Chem. Soc.* **1998**, *120*, 5741.
(58) Gu, X. B.; Guo, Y.; Chan, H.; Kawamura, E.; Kaiser, R. I. *Rev. Sci. Instrum.* **2005**, *76*, 116103/1.
(59) Gu, X. B.; Guo, Y.; Kawamura, E.; Kaiser, R. I. *Rev. Sci. Instrum.* **2005**, *76*, 083115/1.
(60) Guo, Y.; Gu, X.; Kaiser, R. I. *Int. J. Mass Spectrosc.* **2006**, *249/250*, 420.
(61) Guo, Y.; Gu, X.; Kawamura, E.; Kaiser, R. I. *Rev. Sci. Instrum.* **2006**, *77*, 034701/1.
(62) Gu, X.; Guo, Y.; Kawamura, E.; Kaiser, R. I. *J. Vac. Sci. Technol., A* **2006**, *24*, 505.

99.9%; Fluka; 550 Torr; $v_p = 770 \pm 30$ ms^{-1}; $S = 8.0 \pm 0.5$) released by a second pulsed valve perpendicularly in the interaction region; the secondary pulsed valve operated at 80 μs pulse widths, -500 V driving voltage, and was opened 40 μs (helium seeded dicarbon beam) and 3 μs (neon seeded dicarbon beam) prior to the pulsed valve in the primary source chamber. To obtain additional information of the reaction dynamics and on the position of the deuterium versus hydrogen loss, partially deuterated 1,3-butadiene molecules (1,1,4,4-D4-1,3-butadiene and 2,3-D2-1,3-butadiene) were also used in the experiments; however, due to the high costs, data were only collected at the corresponding center-of-mass angles. It should be noted that the primary beam contains carbon atoms and tricarbon molecules as well. However, these species do not interfere with our experiments. Here, the atomic carbon$-$1,3-butadiene reaction products have lower masses than those of the potential C_6H_5 isomers.[63] Previous studies of reactions of tricarbon molecules with unsaturated hydrocarbons like allene and ethylene showed the existence of entrance barriers of at least 45 kJ mol^{-1}, which is higher than our collision energies.[53] Therefore, neither ground-state carbon atoms nor tricarbon molecules interfered with the reactive scattering signal to probe the formation of C_6H_5 isomers.

The reactively scattered species were monitored using a quadrupole mass spectrometric detector in the time-of-flight (TOF) mode after electron-impact ionization of the neutral molecules at 80 eV electron energy. This detector can be rotated within the plane defined by the primary and the secondary reactant beams to allow taking angular resolved TOF spectra. At each angle, up to 600 000 TOF spectra were accumulated to obtain good signal-to-noise ratios. The recorded TOF spectra were then integrated and normalized to extract the product angular distribution in the laboratory frame (LAB). To collect information on the scattering dynamics, the laboratory data (TOF, angular distribution) were transformed into the center-of-mass reference frame utilizing a forward-convolution routine.[64,65] This iterative method initially assumes the angular flux distribution, $T(\theta)$, and the translational energy flux distribution, $P(E_T)$, in the center-of-mass system (CM). Laboratory TOF spectra and the laboratory angular distributions (LAB) were then calculated from the $T(\theta)$ and $P(E_T)$ function and were averaged over a grid of Newton diagrams. Finally, this procedure produces a flux contour map, $I(\theta,u) = P(u) \times T(\theta)$, which plots the flux of the reactively scattered products (I) as a function of the center-of-mass scattering angle (θ) and product velocity (u). Thus, it can be seen as the image of the chemical reaction and contains all of the information on the scattering process.

Finally, it is important to address the electronic states of the dicarbon molecules. Because of the low energy gap between the ground and first excited triplet states (718 cm^{-1}), the supersonic ablation beams likely contain dicarbon in its $X^1\Sigma_g^+$ electronic ground state as well as in its first electronically excited $a^3\Pi_u$ state.[50] For instance, crossed molecular beam reactions of dicarbon molecules with hydrogen sulfide (H_2S) and hydrogen cyanide (HCN) form the HCCS ($X^2\Pi_\Omega$)[66] and CCCN ($X^2\Sigma^+$)[67] products only on the singlet surfaces. The corresponding reactions of triplet dicarbon are either repulsive (hydrogen sulfide reaction) or hold a significant entrance barrier of about 30 kJ mol^{-1} (hydrogen cyanide). Therefore, those crossed beam reactions provided direct evidence that dicarbon molecules in their $X^1\Sigma_g^+$ electronic ground state do exist in the ablation beams. On the basis of the collision-energy dependent shapes of the center-of-mass angular and translational energy distributions extracted from dicarbon-unsaturated hydrocarbon scattering experiments,[49,50,68] the authors inferred that dicarbon molecules also exist in their first electronically excited $a^3\Pi_u$ state. However, because of the narrow energy gap of the ground and excited states, an explicit confirmation based on the experimental reaction energies has remained elusive so far. Therefore, in the present investigation, we also conducted a laser-induced fluorescence (LIF) characterization of the dicarbon beam to probe the dicarbon molecules in the first electronically excited state via the Swan transition ($d^3\Pi_g - a^3\Pi_u$). A schematic setup of the LIF experiment is shown in Figure 1. Triplet dicarbon was excited by the fundamental output of a Lambda Physics Scanmate dye laser using Coumarin 503 dye at about 516.5 nm at laser power of 45 μJ per pulse. The dye laser itself was pumped by an integrated Nd:YAG laser operating at 355 nm at 10 Hz with an output power of 50 mJ per pulse. The dye laser was fired around 200 μs after the pulse valve opening with a pulse energy of a few μJ to intercept the peak of the dicarbon beam. The fluorescence was detected by a Hamamatsu R955 PMT filtered by an Andover band-pass filter (centered at 560 nm with 10 nm bandwidth). The signal was then amplified by a built-in amplifier of the Hamamatsu C7247 PMT socket assembly prior to feeding into a digital oscilloscope and a computer for data collecting and processing. The LIF spectra were then analyzed utilizing a diatomic spectral simulation program by Tan[69] with spectroscopic constants taken from Bernath.[70,71]

3. Electronic Structure and Statistical Calculations

Geometries of various local minima and transition states on the singlet and triplet PESs for the $C_2(X^1\Sigma_g^+/a^3\Pi_u)$ + 1,3-butadiene reactions were optimized using the hybrid density functional B3LYP[72,73] method with the 6-311G** basis set. Vibrational frequencies and molecular structural parameters computed at this B3LYP/6-311G** level of theory were utilized to obtain zero-point energy (ZPE) corrections, to characterize the stationary points, and to perform RRKM computations of reaction rate constants. To refine relative energies of various species, we applied the G3(MP2,CC)//B3LYP version[74,75] of the original Gaussian 3 (G3) scheme.[76] The final energies at 0 K were obtained using the B3LYP optimized geometries and ZPE corrections according to eq 7. Here, $\Delta E_{MP2} = E$[MP2/G3large] $- E$[MP2/6-311G(d,p)] is the basis set correction, and E(ZPE) is the zero-point energy. ΔE(SO), a spin$-$orbit correction, and ΔE(HLC), a higher level correction, from the original G3 scheme were not included in our calculations, as they are not expected to make significant contributions into relative energies. All DFT and MP2 calculations were carried out using the Gaussian 98[77] package, whereas the MOLPRO 2002[78] program package was used to calculate spin-restricted (R) CCSD(T) energies.

$$E_0[\text{G3(MP2,CC)}] = E[\text{CCSD(T)/6-311G(d,p)}] + \Delta E_{MP2} + E(\text{ZPE}) \quad (7)$$

(63) Hahndorf, I.; Lee, H. Y.; Mebel, A. M.; Lin, S. H.; Lee, Y. T.; Kaiser, R. I. *J. Chem. Phys.* **2000**, *113*, 9622.
(64) Vernon, M. Ph.D., University of California, Berkeley, 1981.
(65) Weiss, M. S. Ph.D., University of California, Berkeley, 1986.
(66) Kaiser, R. I.; Yamada, M.; Osamura, Y. *J. Phys. Chem. A* **2002**, *106*, 4825.
(67) Gu, X.; Kaiser, R. I.; Mebel, A. M.; Kislov, V. V.; Klippenstein, S. J.; Harding, L. B.; Liang, M. C.; Yung, Y. L. *Astrophys. J.* **2009**, *701*, 1797.
(68) Zhang, F.; Kim, S.; Kaiser, R. I.; Mebel, A. M. *J. Phys. Chem. A* **2009**, *113*, 1210.
(69) Tan, X. *CyberWit*, 1.4 ed.; Santa Clara, CA, 2004.
(70) Prasad, C. V. V.; Bernath, P. F. *Astrophys. J.* **1994**, *426*, 812.
(71) Tanabashi, A.; Hirao, T.; Amano, T.; Bernath, P. F. *Astrophys. J., Suppl. Ser.* **2007**, *169*, 472.
(72) Becke, A. D. *J. Chem. Phys.* **1993**, *98*, 5648.
(73) Lee, C.; Yang, W.; Parr, R. G. *Phys. Rev. B: Condens. Matter Mater. Phys.* **1988**, *37*, 785.
(74) Curtiss, L. A.; Raghavachari, K.; Redfern, P. C.; Baboul, A. G.; Pople, J. A. *Chem. Phys. Lett.* **1999**, *314*, 101.
(75) Baboul, A. G.; Curtiss, L. A.; Redfern, P. C.; Raghavachari, K. *J. Chem. Phys.* **1999**, *110*, 7650.
(76) Curtiss, L. A.; Raghavachari, K.; Redfern, P. C.; Rassolov, V.; Pople, J. A. *J. Chem. Phys.* **1998**, *109*, 7764.

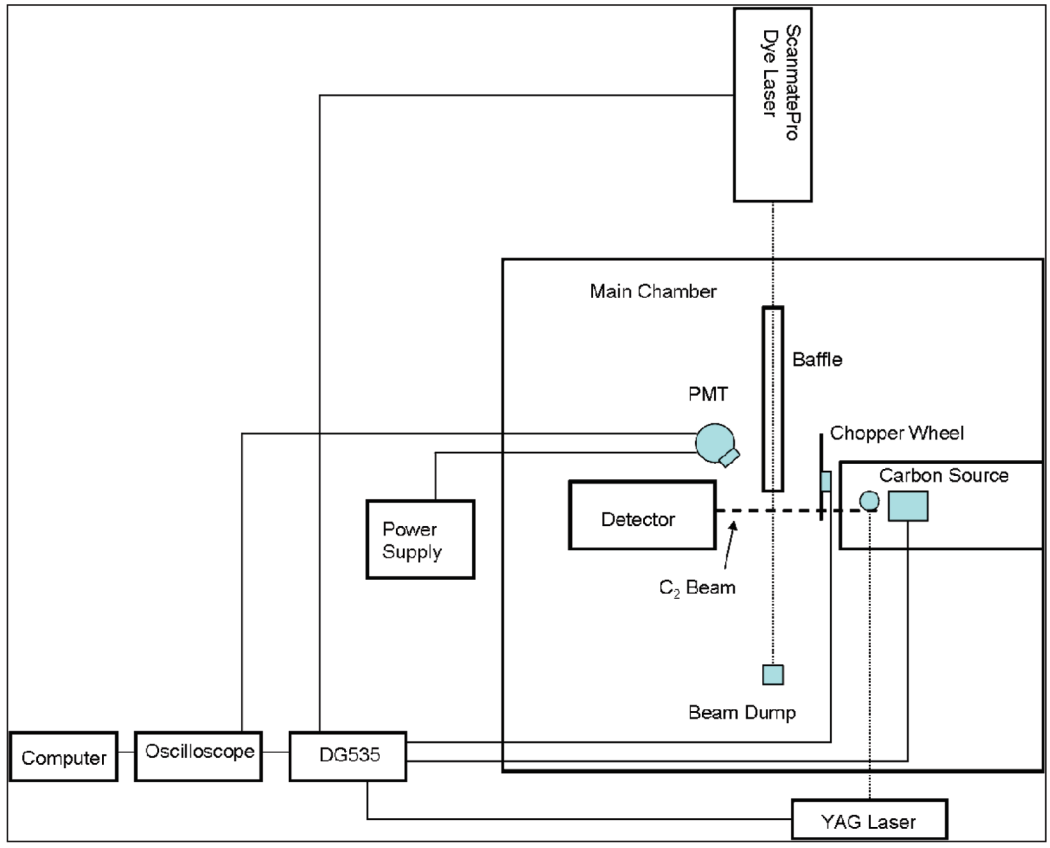

Figure 1. Block diagram of the laser-induced fluorescence (LIF) setup.

Relative yields of various reaction products under single-collision conditions were evaluated by Rice−Ramsperger−Kassel−Marcus (RRKM) calculations[79−81] of energy-dependent rate constants for individual unimolecular steps and of branching ratios of different channels. The computational procedure for these calculations has been described in detail in our previous works.[82] Briefly, we calculated rate constants as functions of the available internal energy of each intermediate or transition state; the internal energy was taken as a sum of the energy of chemical activation and the collision energy, assuming that a dominant fraction of the latter is converted to the internal vibrational energy. Only a single total-energy level was considered throughout, as for single-collision conditions (zero-pressure limit). The harmonic approximation was used in calculations of numbers and densities of states required for evaluating the rate constants. For the reaction channels, which do not exhibit exit barriers, such as H atom eliminations from various singlet C_6H_6 intermediates occurring by a cleavage of single C−H bonds or dissociation to two propargyl radicals by a C−C bond rupture, we applied the microcanonical variational transition state theory (VTST)[79−81] and thus determined variational transition states and rate constants. In microcanonical VTST, the minimum in the rate constant is found along the reaction path according to eq 8:

$$\frac{dk(E)}{dq^{\#}} = 0 \tag{8}$$

where $q^{\#}$ is the reaction coordinate (for instance, the length of the breaking C−H or C−C bond), so that different transition states are found for different available energies. The individual microcanonical rate constants computed using RRKM were thus minimized along the reaction path. These calculations require values of the classical potential energy, zero-point energy, and vibrational frequencies as functions of the reaction coordinate. The details of the procedure for the VTST calculations have been also described earlier.[82] With all rate constants available, we then computed product branching ratios by solving first-order kinetic equations for unimolecular decomposition of the initial adducts in the $C_2(X^1\Sigma_g^+/a^3\Pi_u)$ plus 1,3-butadiene reactions using the steady-state approximation under the assumption that the internal energy is completely randomized.

4. Results

4.1. Laboratory Data. For the dicarbon−1,3-butadiene reaction, reactive scattering signal was monitored in the range of mass-to-charge ratios, m/z, from 77 ($C_6H_5^+$) to 72 (C_6^+). At each angle, the time-of-flight (TOF) spectra of these ions were, after scaling, superimposable, suggesting that signal at lower m/z ratios originated from dissociative ionization of the C_6H_5 parent molecules in the electron impact ionizer. The observation of signal $m/z = 77$ alone implies that the dicarbon versus hydrogen atom exchange pathway yielding C_6H_5 isomer(s) is

(77) Frisch, M. J.; et al. *Gaussian 98*, revision A11; Gaussian, Inc.: Pittsburgh, PA, 2001. Details can be found in the Supporting Information.
(78) Werner, H. J.; et al. *MOLPRO*, Version 2002, a package of ab initio program, 2002; see http://www.molpro.net.
(79) Eyring, H.; Lin, S. H.; Lin, S. M. *Basis Chemical Kinetics*; Wiley: New York, 1980.
(80) Robinson, P. J.; Holbrook, K. A. *Unimolecular Reactions*; Wiley: New York, 1972.
(81) Steinfeld, J. I.; Francisco, J. S.; Hase, W. L. *Chemical Kinetics and Dynamics*, 2nd ed.; Prentice Hall: Engelwood Cliffs, NJ, 1999.
(82) Kislov, V. V.; Nguyen, T. L.; Mebel, A. M.; Lin, S. H.; Smith, S. C. *J. Chem. Phys.* **2004**, *120*, 7008.

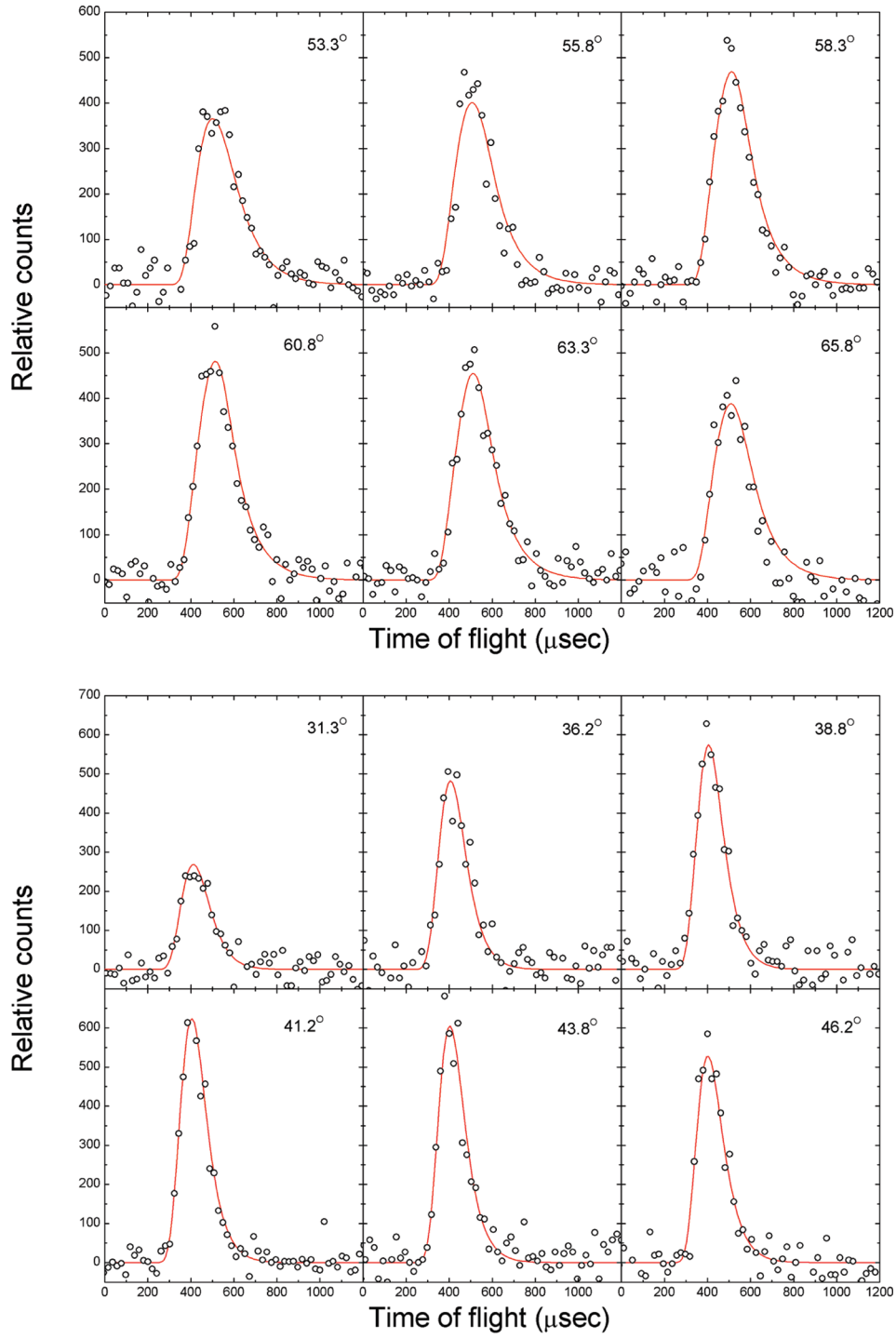

Figure 2. Time-of-flight data recorded at $m/z = 76$ ($C_6H_4^+$), that is, a fragment ion of C_6H_5, for the reaction of dicarbon $C_2(X^1\Sigma_g^+/a^3\Pi_u)$ with 1,3-butadiene $CH_2CHCHCH_2(X^1A_g)$ at various laboratory angles at collision energies of 12.7 (top) and 33.7 kJ mol^{-1} (bottom). The circles represent the experimental data, and the solid lines are the fits. Each TOF spectrum has been normalized to the relative intensity of each angle.

open. Complete TOF and laboratory angular distributions were recorded at $m/z = 76$ ($C_6H_4^+$) because of the highest signal-to-noise ratio at this mass-to-charge ratio (Figures 2 and 3). The corresponding LAB distributions are shown in Figure 3. Note that even at the higher collision energy, the laboratory angular distribution of the heavy reaction products with the generic formula C_6H_5 is forward−backward symmetric, peaks around 42.5° close to the center-of-mass angle 43°, and is spread at least 50° within the scattering plane. This shape of the LAB distribution suggests that the reaction proceeds likely via indirect scattering dynamics involving C_6H_6 reaction intermediate(s). Having identified the atomic hydrogen loss pathway, it is important to derive experimentally to what extent the hydrogen atom originates from the terminal methylene group (CH_2) and/or from the methylidyne group (CH) at the C2/C3 carbon atoms. Therefore, we conducted crossed beam experiments with 1,1,4,4-D4-1,3-butadiene and 2,3-D2-1,3-butadiene. In case of 2,3-D2-1,3-butadiene, signal was monitored at $m/z = 79$ ($C_6H_3D_2^+$), indicating the presence of the dicarbon versus atomic hydrogen loss, in which the hydrogen atom originated from the terminal

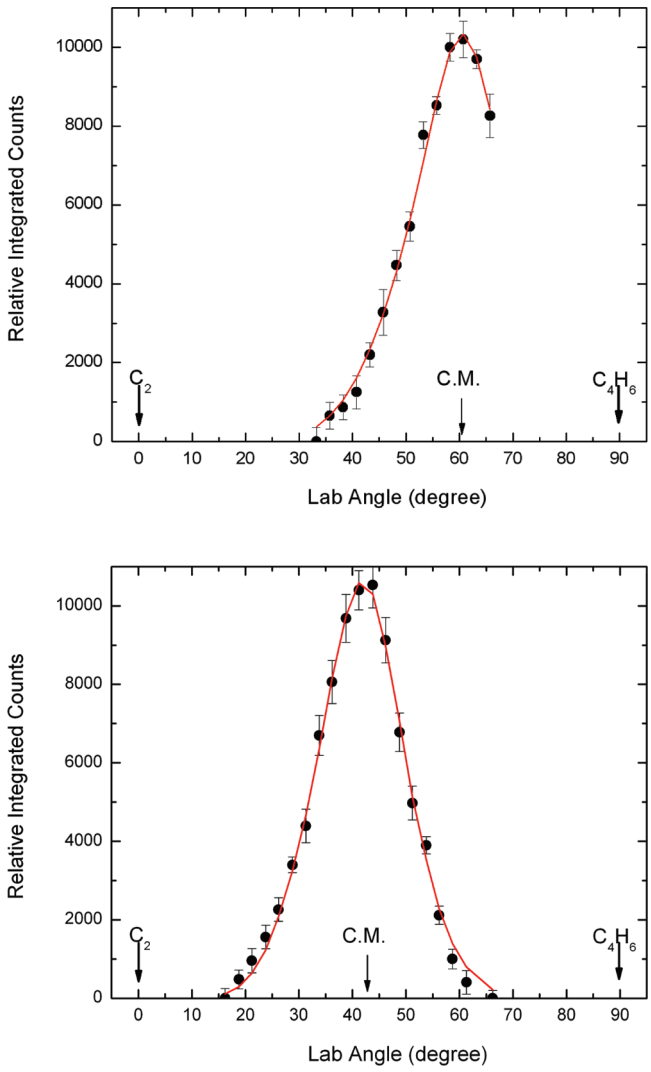

Figure 3. Laboratory angular distributions (LAB) of the C_6H_5 product recorded at its fragment ion of $m/z = 76$ ($C_6H_4^+$) at collision energies of 12.7 kJ mol^{-1} (top) and 33.7 kJ mol^{-1} (bottom) for the reaction of dicarbon $C_2(X^1\Sigma_g^+/a^3\Pi_u)$ with 1,3-butadiene $CH_2CHCHCH_2(X^1A_g)$. Circles and error bars indicate experimental data, and the solid lines are the calculated distributions with the best-fit center-of-mass functions. C.M. indicates the center-of-mass angle.

(C1/C4) carbon atoms. Considering the reaction with 1,1,4,4-D4-1,3-butadiene, we monitored signal at $m/z = 81$ ($C_6HD_4^+$), suggesting that the hydrogen atom can be also emitted from the central C2/C3 positions of the 1,3-butadiene molecule. Note that signal at $m/z = 79$ is much stronger than that at $m/z = 81$ by a factor of about 3 (Figure 4). This finding suggests that in the corresponding dicarbon−1,3-butadiene reaction, the departing hydrogen atom originates mainly from the terminal methylene group and to a smaller extent from the central methylidyne group. Note, however, that part of the signal at $m/z = 81$ may also originate from the $^{13}CC_5D_3H_2^+$ ion (formed after ionization of the $^{13}CC_5D_3H_2$ parent, which in turn was generated via atomic deuterium loss from the CD_2 groups), which should have a 6.6% natural abundance.

4.2. Center-of-Mass Functions. Figure 5 displays the center-of-mass translational energy, $P(E_T)$, together with center-of-mass angular distributions, $T(\theta)$'s, for both collision energies. First, we would like to stress that the laboratory data could be fit at both collision energies with a single channel of the mass combination 77 amu (C_6H_5) and 1 amu (H). Best fits of the LAB distributions and the TOF data could be achieved with $P(E_T)$'s extending to a maximum translational energy release (E_{max}) of 355 ± 25 kJ mol^{-1} (lower collision energy) and 365 ± 25 kJ mol^{-1} (higher collision energy). Recall that E_{max} presents the sum of the reaction exoergicity plus the collision energy. Therefore, by subtracting the collision energy from the high energy cutoffs, we are left with an experimental exoergicity of 337 ± 30 kJ mol^{-1} averaged over both collision energies. These experimental derived data can be compared at a later stage with ab initio calculations to identify the nature of the structural isomer(s) formed. Second, both $P(E_T)$'s were found to have a broad peak from near zero to about 35−45 kJ mol^{-1} translational energy; this pattern likely indicates the existence of multiple exit channels (one from the singlet and a second one from the triplet surface),[51,83] which involve at least one tight exit transition state and hence a repulsive energy loss in the atomic hydrogen loss emission.

We would like to comment now on the center-of-mass angular distributions. The $T(\theta)$'s at higher and lower collision energies depict similar patters: both distributions showed flux over the complete angular range and were found, within the error limits, to be forward−backward symmetric with respect to 90°. Ratios of the flux intensities at 0° versus 90° were found to be 1.3 ± 0.2 and 2.4 ± 0.8 for the lower and higher collision energy, respectively. These characteristics indicate that this reaction follows indirect scattering dynamics via the formation of C_6H_6 intermediates.[84] Also, the forward−backward symmetry implies that the lifetime of the decomposing complex(es) is longer than the rotational period.[85] Finally, the sideways scattering (maxima at 90°) indicates geometrical constraints of the decomposing complex, here a preferential hydrogen atom ejection perpendicular to the molecular plane of the decomposing C_6H_6 moiety almost parallel to the total angular momentum vector.[86] The above characteristics are also revealed in the flux contour maps (Figure 6). At both collision energies, the flux distributions are forward−backward symmetric and show a sideways-scattering pattern.

4.3. LIF Spectra of the Dicarbon $d^3\Pi_g - a^3\Pi_u$ Swan System. We also characterized the rovibrational state populations of triplet dicarbon in those parts of the dicarbon beam, which intersect the 1,3-butadiene beam, by taking the laser-induced fluorescence (LIF) spectra of the (0,0) and (1,1) bands of the Swan transition. We estimated the rovibrational populations by comparing experimental LIF spectra with simulated fits utilizing a diatomic spectral simulation program by Tan;[69] spectroscopic constants were taken from Bernath.[70,71] Figure 7 shows the measured and simulated spectra for ablated dicarbon cooled in supersonic expansion of neon and helium carrier gas. The fitting parameters for the simulated spectra are the vibrational populations and rotational temperatures for $v = 0$ and $v = 1$. For the cooled part of the beam, the estimated vibrational populations and rotational temperatures are compiled in Table 2. However, besides the well-defined spectral structure of the cooled molecules, we also observed spectral features corresponding to noncooled species. As compared to the (0,0) band, the weaker (1,1) band is effected more significantly by "hot" dicarbon lines. Note that the population of $v = 1$ in triplet dicarbon beam is

(83) Gu, X.; Guo, Y.; Zhang, F.; Kaiser, R. I. *J. Phys. Chem. A* **2007**, *111*, 2980.
(84) Levine, R. D. *Molecular Reaction Dynamics*; Cambridge University Press: Cambridge, UK, 2005.
(85) Miller, W. B.; Safron, S. A.; Herschbach, D. R. *Discuss. Faraday Soc.* **1967**, *No. 44*, 108.
(86) Bettinger, H. F.; Kaiser, R. I. *J. Phys. Chem. A* **2004**, *108*, 4576.

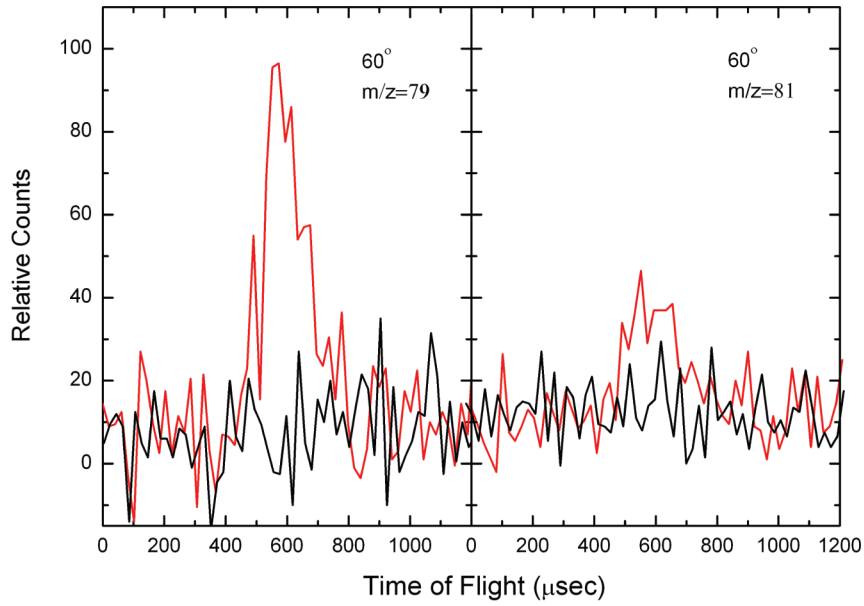

Figure 4. Left: Time-of-flight spectrum recorded close to the center-of-mass angles at $m/z = 79$ ($C_6H_3D_2^+$) during the reaction of dicarbon $C_2(X^1\Sigma_g^+/a^3\Pi_u)$ with 2,3-D2-1,3-butadiene. Right: TOF spectrum recorded at $m/z = 81$ ($C_6HD_4^+$; $^{13}CC_5D_3H_2^+$) in the crossed beam reaction of dicarbon $C_2(X^1\Sigma_g^+/a^3\Pi_u)$ with 1,1,4,4-D4-1,3-butadiene. The red lines are the data with the ablation laser "on"; the black lines depict the background signal with the ablation laser "off".

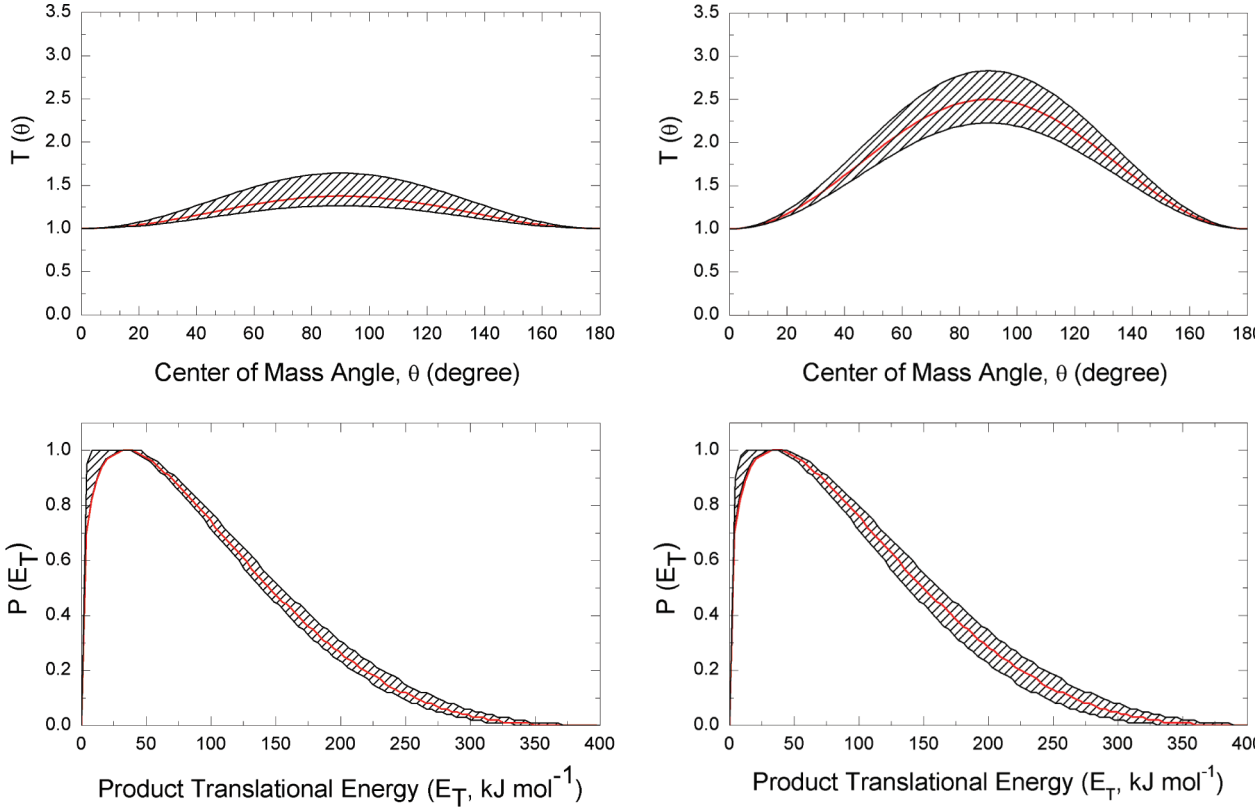

Figure 5. Center-of-mass angular (top) and translational energy flux distributions (bottom) of the reaction of dicarbon $C_2(X^1\Sigma_g^+/a^3\Pi_u)$ with 1,3-butadiene $CH_2CHCHCH_2(X^1A_g)$ at collision energies of 12.7 (left) and 33.7 kJ mol^{-1} (right). Hatched areas indicate the acceptable upper and lower error limits of the fits. The red line defines the best-fit functions.

25% (helium) to 38% (neon), that is, similar to a fraction of 0.35 obtained by Casavecchia et al. in continuous dicarbon beams.[87] However, two significant differences exist. Whereas in our beam the vibrational population changes with the carrier gas from 0.25 to 0.38, Casavecchia's vibrational population is invariant on the carrier gas. Also, we do not have evidence of vibrational states higher than $v = 1$, whereas Casavecchia detects vibrational populations as high as $v = 4$. Finally, the rotational temperatures in our beam were found to be slightly lower (210 and 190 K in helium and neon for $v = 0$, respectively) as compared to 250 and 200 K in Casavecchia's study. This is likely the effect of the lower backing pressure (225 Torr) and

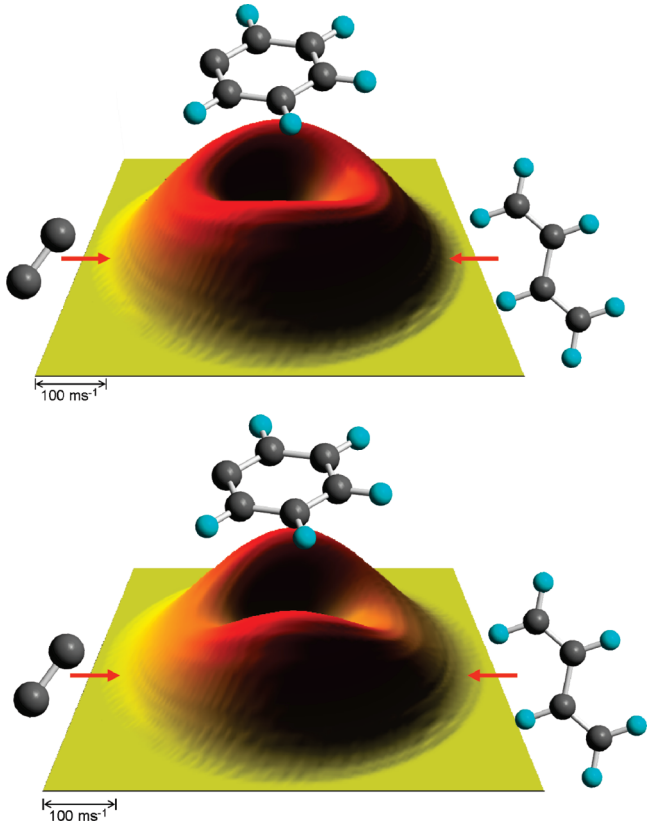

Figure 6. Flux contour maps of the reactions of dicarbon $C_2(X^1\Sigma_g^+/a^3\Pi_u)$ with 1,3-butadiene $CH_2CHCHCH_2(X^1A_g)$ derived from the best-fit functions (Figure 5) at collision energies of 12.7 (top) and 33.7 kJ mol^{-1} (bottom).

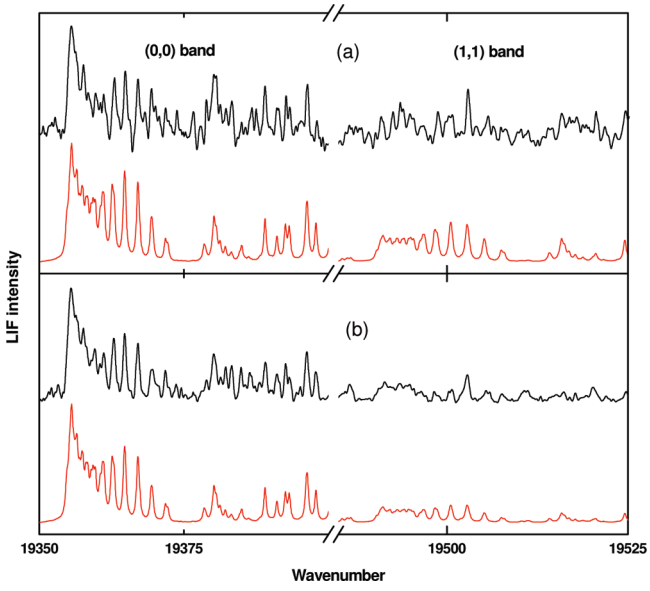

Figure 7. LIF spectra of the (0,0) and (1,1) bands in the Swan system of $C_2(a^3\Pi_u)$ cooled in neon (a) and helium (b) carrier gas. The solid lines depict the recorded spectra; the red lines are offset for clarity and present the best-fit simulations.

hence lower cooling efficiency in the continuous sources as compared to pulsed sources with backing pressures of 3040 Torr utilized in the present, pulsed experiments. To summarize, our

Table 2. Vibrational (v) Populations and Rotational Temperatures of Supersonically Cooled Triplet Dicarbon Molecules

	v			
	neon seeded		helium seeded	
	0	1	0	1
population	0.62 ± 0.08	0.38 ± 0.08	0.75 ± 0.05	0.25 ± 0.05
T_{rot}, K	190 ± 10	140 ± 20	210 ± 10	180 ± 20

LIF measurements clearly indicate the presence of dicarbon molecules in their first electronically excited triplet state.

5. Discussion

The results of the crossed molecular beam experiments showed that the reaction of dicarbon with 1,3-butadiene is formally dictated by a replacement of atomic hydrogen by a dicarbon unit leading to a product of the gross formula C_6H_5. The next step is to determine which isomer(s) are being formed. To answer this question, we compare the experimentally derived reaction energy of 337 ± 30 kJ mol^{-1} with computed data for distinct isomers (Figure 8). Our electronic structure calculations revealed that reactions to form the phenyl radical plus atomic hydrogen are exoergic by 368 ± 10 and 379 ± 10 kJ mol^{-1} on the singlet and triplet surfaces, respectively. Within the experimental and theoretical error limits, both the experimental and the theoretical data suggest the formation of the phenyl radical. The computations identified also pathways to five acyclic C_6H_5 products (**p1**−**p5**). Their reaction exoergicities range from 57 to 183 kJ mol^{-1}. It is obvious that these data do not correlate well with the experimentally derived energetics of 337 ± 30 kJ mol^{-1}. Therefore, the phenyl radical must account for the high energy cutoff of the center-of-mass translational energy distributions. However, based on the experimental data alone, smaller contributions of the energetically less stable, acyclic isomers **p1**−**p5** cannot be ruled out at the present stage.

What are the reaction dynamics leading to the phenyl radical? Let us focus on the triplet surface first. Here, the phenyl radical can be formed via indirect scattering dynamics, as verified from the center-of-mass angular distributions, by decomposition of intermediates **t-i4** and/or **t-i3**. Both structures are interconnected by an isomerization barrier of 194 kJ mol^{-1} with respect to **t-i3**. The geometry of both exit transition states to form phenyl plus atomic hydrogen suggests that the hydrogen atom is leaving perpendicularly within the plane of the rotating complex (Figure 9). This was also derived from the "sideways" peaking of the center-of-mass angular distribution. Considering **t-i4**, this could be understood if we look at the reverse reaction of atomic hydrogen plus phenyl radical. To form triplet benzene, the hydrogen atom does not attack the σ radical site to form a bond; in such a case, a singlet state would be produced. Instead, the π system of phenyl is attacked to break the aromatic system; two unpaired electrons then end up in the π system. The fragmenting complex **t-i3** could also account for the experimental finding of a "sideways scattering". Here, the geometry of the transition state (Figure 9) indicates that the hydrogen atom leaves almost perpendicularly to the molecular plane of the decomposing intermediate **t-i3** via a tight exit transition state located 27 kJ mol^{-1} above the separated products. Because this addition proceeds to a closed-shell electronic system (the

(87) Leonori, F.; Petrucci, R.; Hickson, K. M.; Segoloni, E.; Balucani, N.; Le Picard, S. D.; Foggi, P.; Casavecchia, P. *Planet. Space Sci.* **2008**, *56*, 1658.

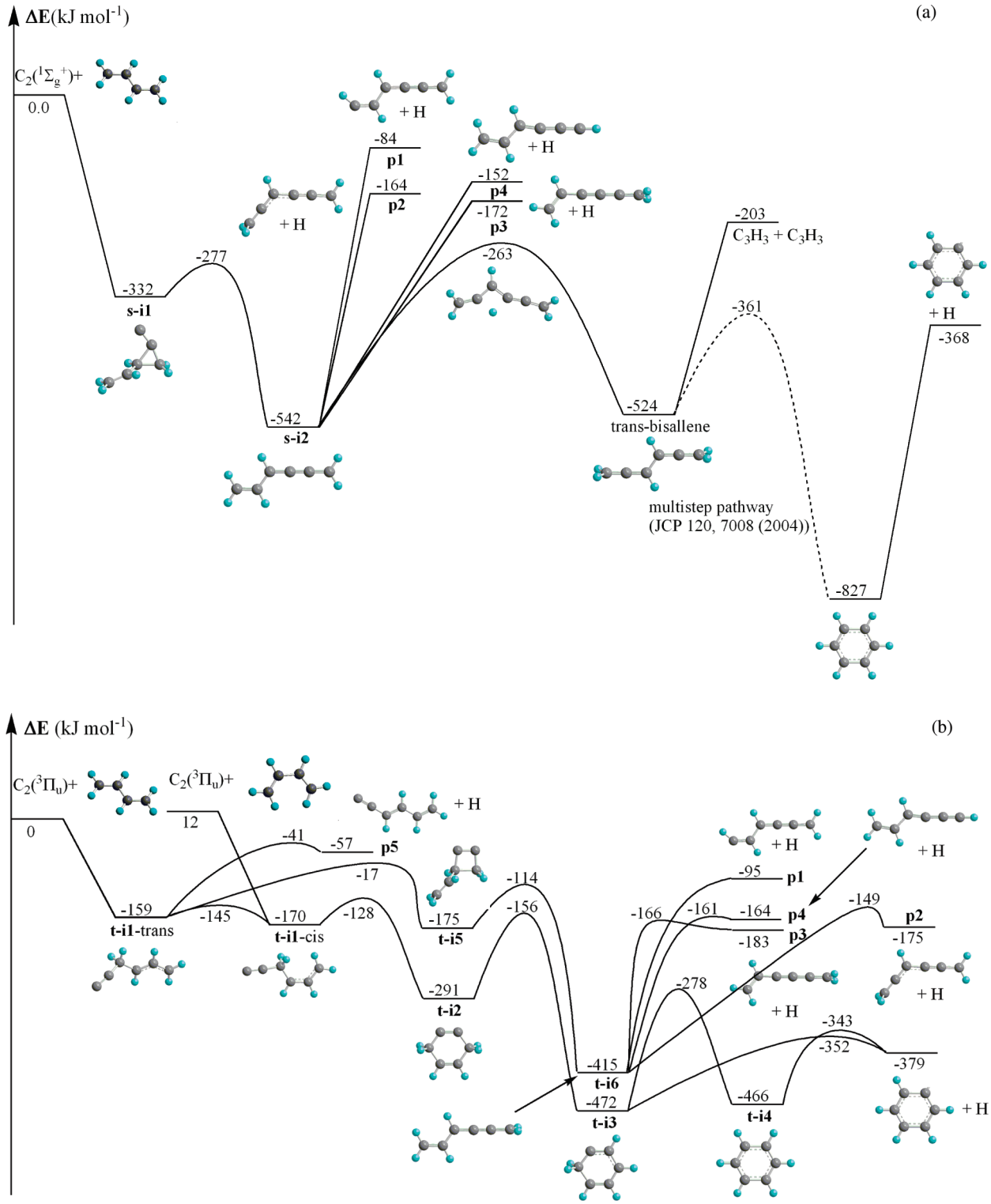

Figure 8. Potential energy surfaces (PESs) of the reactions of ground-state dicarbon $C_2(X^1\Sigma_g^+)$ (a) and excited-state dicarbon $C_2(a^3\Pi_u)$ (b) with 1,3-butadiene $CH_2CHCHCH_2$ (X^1A_g) to form various C_6H_5 isomers plus atomic hydrogen. Energies are given in kJ mol^{-1}.

unpaired electron of the phenyl radical is located inside the molecular plane in an A_1 orbital), the derived barrier height to addition of 27 kJ mol^{-1} is reasonable and compares well with barriers of hydrogen atom addition processes to closed-shell olefins and alkynes. For completeness, we also have to investigate the singlet surface. Here, only the benzene molecule was found to be able to decompose to phenyl plus atomic hydrogen. However, the hydrogen atom leaves within the molecular plane of the decomposing benzene molecule via a simple bond rupture process (the reversed atom−radical recombination at the radical centers to form benzene has no entrance barrier). Therefore, this process should lead to a center-of-mass angular distribution peaking at the poles (0° and 180°), but not at 90° as found experimentally. Consequently, we may conclude that the phenyl radical is predominantly formed on the triplet manifold via **t-i3** and/or **t-i4**.

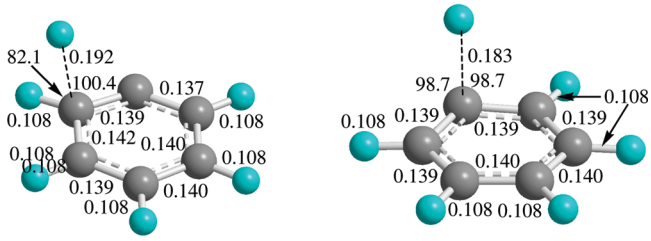

Figure 9. Computed geometries of the transition states involved in the decomposition of **t-i3** (left) and **t-i4** (right) to the phenyl radical plus atomic hydrogen. Bond angles are given in degrees, and bond distances are in nanometers (nm).

Therefore, we are proposing the following reaction dynamics on the triplet surface: the dicarbon molecule $C_2(a^3\Pi_u)$ adds without barrier to the terminal carbon atom of the 1,3-butadiene molecule, yielding intermediate **t-i1** trans. The latter isomerizes easily to the corresponding cis form, which then rearranges via ring closure to **t-i2**. The latter undergoes a hydrogen shift to **t-i3**, which then fragments via atomic hydrogen loss through a tight exit transition state to the phenyl radical plus atomic hydrogen. Alternatively, **t-i3** could isomerize to **t-i4** before emitting a hydrogen atom. In total, the formation of the phenyl radical involves, after the initial addition, at least three isomerization steps. Because the center-of-mass angular distributions at both collision energies were found to be forward−backward symmetric, these isomerization steps are faster than at least one rotational period of the decomposing complex(es) **t-i3** and/or **t-i4**. The proposed reaction mechanism is also in line with the isotopically labeled experiments. The much stronger signal for the hydrogen loss channel observed in the reaction with 2,3-D2-1,3-butadiene as compared to 1,1,4,4-D4-1,3-butadiene strongly suggests that the departing hydrogen atom originates mainly from the terminal methylene group. Indeed, for the phenyl forming via **t-i3**, the departing hydrogen atom does originate solely from the terminal methylene group of 1,3-butadiene at the C1/C4 position. On the other hand, a decomposition of **t-i4** should result in a strong reactive scattering signal of the atomic hydrogen loss in the reaction with 1,1,4,4-D4-1,3-butadiene. This strong scattering signal was clearly not observed experimentally. Therefore, we may conclude that comparing **t-i3** with **t-i4**, **t-i3** presents likely the dominant fraction of the decomposing complexes forming the phenyl radical plus atomic hydrogen. This is confirmed in RRKM calculations. First, the results show that on the triplet surface, phenyl is almost the exclusive reaction product with fractions of 99.34% and 98.30% at lower and higher collision energies of 13.2 and 34.7 kJ mol^{-1}, respectively. Here, 96−98% of the phenyl radical was found to be formed via decomposition of **t-i3**. These findings are fully consistent with our proposed reaction mechanism. To summarize, both the experimental and the theoretical investigations correlate nicely and suggest that, on the triplet surface, the phenyl radical is formed via a five-step pathway through a barrierless addition and consecutive isomerization steps including ring closure and hydrogen migration followed by a decomposition of the intermediate **t-i3** through a tight exit transition state.

However, if only the triplet surface is involved, we should have derived center-of-mass translational energy distributions peaking well away from zero translational energy. This is clearly not the case. Both distributions have rather broad distribution maxima ranging from zero to 35−45 kJ mol^{-1}. This pattern is characteristic of multiple exit channels, typically in which one transition state is tight, and a second one is rather loose.[49−51] Therefore, having identified the reaction pathway on the triplet surface to form the phenyl radical, we are turning our attention now to the singlet manifold. Here, the formation of a significant amount of the phenyl radical was dismissed due to two facts: the experimentally found sideways peaking of the center-of-mass angular distributions and the much stronger signal for the hydrogen loss channel observed in the reaction with 2,3-D2-1,3-butadiene as compared to 1,1,4,4-D4-1,3-butadiene (see above). Which of the structural isomers **p1**−**p4** could account for the hydrogen loss pathway? Note that, on the basis of the electronic structure calculations, $C_2(X^1\Sigma_g^+)$ adds without an entrance barrier to one of the carbon−carbon double bonds of 1,3-butadiene to form a cyclic intermediate **s-i1**. This intermediate then undergoes ring-opening to an acyclic intermediate **s-i2**. Electronic structure calculations predicted that the latter can decompose to **p1** and **p4** via hydrogen atom losses from the terminal carbon atoms of **s-i2** or to **p2** and **p3** through atomic hydrogen ejection from the center carbon atoms of **s-i2**. In case of the 1,1,4,4-D4-1,3-butadiene reactant and the observation of the atomic hydrogen loss connected to the two central carbon atoms, this would translate into the formation of **p2** and/or **p3** via loose exit transition states involving simple bond rupture processes.

Table 3. Calculated Product Branching Ratios (in %) for the $C_2(X^1\Sigma_g^+)$ + $CH_2CHCHCH_2$ (X^1A_g) Reaction at Various Collision Energies

	E_{col}, kJ mol^{-1}		
	0	13	34
phenyl + H	41.2	32.3	21.1
C_3H_3 + C_3H_3	31.3	33.9	35.4
p2 + H	8.5	10.8	14.6
p3 + H	13.5	16.1	20.1
p4 + H	5.5	6.9	8.8

The overall reaction exoergicities to form **p2** and **p3** were computed to be 164 and 172 kJ mol^{-1}, respectively. The formation of these molecules could also account for the part of the translational energy distribution peaking close to zero translational energy. Note that, in principle, **p2** and **p3** could also be formed on the triplet surface; however, the corresponding exit transition states are rather tight. Also, recall that phenyl radical was computed to be almost the exclusive product on the triplet manifold. Therefore, on the singlet surface, the hydrogen emission from the decomposing complex is found to be barrierless, which results in a $P(E_T)$ peaking near zero kinetic energy. However, on the triplet manifold, the formation of phenyl radical involved an exit barrier of 27 kJ mol^{-1}; this in turn causes the $P(E_T)$ peaking away from the zero translational energy. The involvement of both the singlet and the triplet surfaces is therefore suggested to lead to a combination of both features (peaking close to zero and away from zero translational energy) and hence a broad plateau-like distribution maxima. This broad plateau was also observed in the crossed beam reactions of ground- and excited-state dicarbon molecules with acetylene and ethylene.

Similar to the triplet surface, we also conducted RRKM calculations on the singlet manifold. The results of RRKM calculations of product branching ratios on the singlet PES are collected in Table 3. They show that, in the case of statistical behavior, about one-third of the total reaction products should be propargyl radicals formed by the single C−C bond cleavage in *trans*-bisallene; due to the significant background at m/z =

39 from the 1,3-butadiene reactant, we could not probe the formation of the propargyl radical experimentally. The yield of the phenyl radical would constitute about 41% at zero collision energy, but rapidly decreases to 32% and 21% at collision energies of 13 and 34 kJ mol^{-1}, respectively. On the contrary, the yield of the acyclic isomers **p2**−**p4** increases with collision energy to a total of about 34% and 43% at 13 and 34 kJ mol^{-1}, respectively. Among the acyclic isomers, the energetically most favorable **p3** structure exhibits the highest yield followed by **p2** and **p4**. This is consistent with our experimental studied using partially isotopically labeled 1,3-butadienes. It should be noted, however, that the pathway to phenyl on the singlet surface is complicated and multistep and would be favored only if a complete statistical equilibration takes place. However, if the energy randomization is incomplete and the energy is still "located" in the initially formed bonds, the production of the acyclic isomers via a barrierless C−H bond cleavage in **s-i2** might be favored.

6. Conclusions

We have conducted crossed molecular beam experiments of dicarbon molecules in their $X^1\Sigma_g^+$ electronic ground state as well as in its first electronically excited $a^3\Pi_u$ state with 1,3-butadiene and two partially deuterated counterparts (1,1,4,4-D4-1,3-butadiene and 2,3-D2-1,3-butadiene) at two collision energies of 12.7 and 33.7 kJ mol^{-1}. These experiments were combined with electronic structure and RRKM calculations on the singlet and triplet C_6H_6 surfaces. Our combined experimental and theoretical investigation suggests that the phenyl radical is formed at least on the triplet surface via indirect scattering dynamics through a long-lived reaction intermediate. Formed by a barrierless addition of triplet dicarbon to one of the terminal carbon atoms of 1,3-butadiene, the collision complex undergoes trans−cis isomerization followed by ring closure and hydrogen migration prior to hydrogen atom elimination forming the phenyl radical. The latter step emits the hydrogen atom almost perpendicularly to the rotational plane of the decomposing intermediate and almost parallel to the total angular momentum vector. On the singlet surface, smaller contributions of the phenyl radical could not be excluded; experiments with partially deuterated 1,3-butadiene suggested the formation of at least the thermodynamically less stable acyclic isomer **p3**. On a final note, we recognize that it is very difficult to pin down the absolute ratio of singlet versus triplet dicarbon in the beam. If triplet dicarbon dominates over singlet dicarbon, and the phenyl radical is formed on the singlet manifold to about 20−30% as extracted from our RRKM calculations, this could smear out the contribution of the phenyl radical on the singlet surface to the shape of the center-of-mass angular distribution. Therefore, we would like to caution that the formation of phenyl on the singlet surface with fractions of 20−30% cannot be ruled out at the present stage. Nevertheless, the synthesis of the phenyl radical on the triplet surface via a five-step pathway involving indirect scattering dynamics is evident. The present results provide the very first experimental evidence of the formation of an aromatic hydrocarbon molecule under single collision conditions in a bimolecular gas-phase reaction of two acyclic molecules at collision energies relevant to combustion flames. Future kinetic models of hydrocarbon flames shall incorporate this new reaction pathway to form phenyl so that an objective comparison on its relevance with previously postulated formation routes to phenyl can be conducted.

Acknowledgment. This work was supported by the U.S. Department of Energy, Basic Energy Sciences (DE-FG02-03ER15411 to the University of Hawaii and DE-FG02-04ER15570 to Florida International University).

Supporting Information Available: Full refs 77 and 78. This material is available free of charge via the Internet at http://pubs.acs.org.

JA908559V